ACTA IMEKO
ISSN: 2221-870X
December 2024, Volume 13, Number 4, 1 - 5

Comparative analysis of physical models of two-electrode conductivity cells with end and lateral liquid supplies

Oleksii Stennik[1]

[1] *Ukrmetrteststandart, 4 Metrologichna St, Kyiv, 03143, Ukraine*

ABSTRACT
This article presents a physical model of a two-electrode conductivity cell with holes for filling located in the electrodes. The study investigates the non-uniformity of the current density distribution within the cell, caused by the presence of these holes. Using the finite element method (FEM), the electrical resistance bias of the cell is calculated and compared to an idealized model - a liquid column with specific geometric dimensions and a uniform field inside. A comparison of the resistance bias values between two models - one with end holes (located in the electrodes) and one with lateral liquid supply - is conducted. The results demonstrate that the resistance bias is highly dependent on the diameter of the holes and is mostly unaffected by their position. In most cases, the resistance bias of the model with holes in the electrodes is 3–6 % lower in absolute value compared to the model with side holes, assuming identical geometric parameters for the cell; meanwhile, the bias signs are opposite for these models.

Section: RESEARCH PAPER

Keywords: Conductometry; two-electrode conductivity cell; resistance bias; finite element analysis

Citation: O. Stennik, Comparative analysis of physical models of two-electrode conductivity cells with end and lateral liquid supplies, Acta IMEKO, vol. 13 (2024) no. 4, pp. 1-5. DOI: 10.21014/actaimeko.v13i4.1763

Section Editor: Leonardo Iannucci, Politecnico di Torino, Italy

Received January 31, 2024; **In final form** November 11, 2024; **Published** December 2024

Corresponding author: Oleksii Stennik, e-mail: metrology@protonmail.com

1. INTRODUCTION

For the practical realization of the unit of electrolytic conductivity (EC) k (S·m^{-1}), national metrology institutes (NMIs) usually use contact two-electrode differential conductivity cells with a clearly defined geometry. Several types of such cells are known: a cell with a removable central section [1]–[7], a piston-type cell [6]–[10], and a differential double cell [11].

The cell with a removable central extension section has gained the greatest popularity among NMIs. Despite the fact that this design was first proposed more than 30 years ago [12], it continues to be replicated in the development of national measurement standards today [3]. The central section of such a cell contains flange connections and can be removed. This ability allows the distance between the electrodes to be changed, thereby changing the electrical resistance of the cell. The operating algorithm is according to the following: First, the cell resistance R_{m1} (Ω) is measured without a central section at a liquid column length of 2 l. The liquid column length is then increased to 2 l + L by placing a central section between the two half-cells, and the resistance R_{m2} (Ω) is measured. EC is expressed as follows [8]-[10]:

$$k = \frac{L}{A}\frac{1}{R_{\mathrm{m2}} - R_{\mathrm{m1}}} = \frac{4\,L}{\pi\,D^2}\frac{1}{R_{\mathrm{m2}} - R_{\mathrm{m1}}}, \quad (1)$$

where A (m^2) is the cross-sectional area, D (m) is the inner diameter of the cell, and L (m) is the length of the "virtual" liquid column. Thus, the principle of realization of the EC unit k (S·m^{-1}) by such a cell is to measure the electrical resistance of a "virtual" liquid column of a clearly defined geometry, provided that there is a uniform current density distribution J (A·m^{-2}).

In reality, for a design containing flanged connections, it is difficult to ensure a uniform current density distribution J (A·m^{-2}) due to the possible radial displacements of the cell sections. The methodological error in measuring using a cell of such a design can reach 0.08 % at a radial displacement of 0.6 mm [13].

The simplest and cheapest option for a primary cell that does not contain flange connections is the two-electrode differential double cell. Structurally, it consists of two cells of different lengths, L_1 (m) and L_2 (m), but the same inner diameter, D (m) (Figure 1). All four electrodes in both cells are fixed, and therefore the liquid columns in such a differential cell have a constant "frozen" geometry. The presence of holes for filling in

(a)

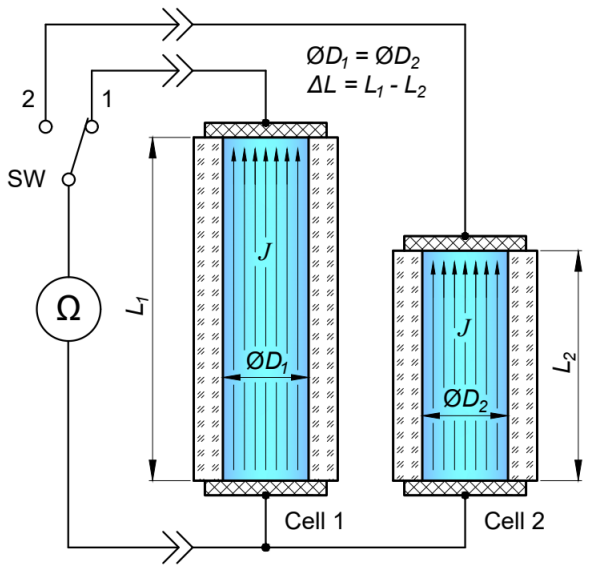

(b)

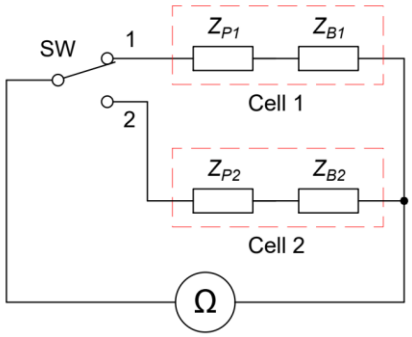

Figure 1. A physical model of a differential conductivity double cell and its equivalent circuit diagram.
(a) A physical model of a differential conductivity double cell;
(b) Equivalent circuit diagram of the differential conductivity double cell (Z_{P1} and Z_{P2} are the polarization impedances of the cells, and Z_{B1} and Z_{B2} are the bulk impedances).

each of the cells results in distortion of the current density distribution J (A·m^{-2}) inside the liquid column. This leads to a bias in the electrical resistance of the filled cell with respect to the resistance of the idealized model with a homogeneous field (without holes) (Figure 2) by a relative value of δ_R (%):

$$\delta_R = \frac{R_w - R_{wo}}{R_{wo}} \cdot 100\,, \tag{2}$$

where R_w (Ω) is the resistance of the cell having holes for filling, and R_{wo} (Ω) is the resistance of the idealized cell model with a homogeneous field inside, calculated as follows [1]:

$$R_{wo} = \frac{L}{A}\frac{1}{k} = \frac{4L}{\pi D^2}\frac{1}{k}. \tag{3}$$

Since the diameter and position of the holes for filling the cell can be measured, the resistance bias δ_R (%) (2) can be theoretically calculated and used as a correction. Such studies were conducted for the cell design with a lateral liquid supply [11]. However, there is another design type where the holes for filling the cell are located in the electrodes, Figure 3(a), hereinafter referred to as model A.

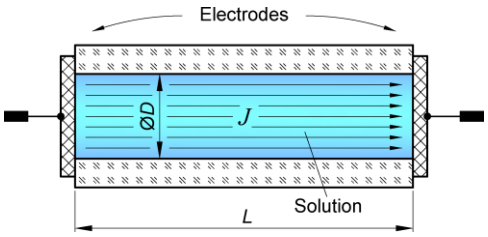

Figure 2. A physical model of an idealized conductivity cell with a homogeneous field inside.

The purpose of this article is to establish quantitative characteristics of the error in measuring the resistance of the cell with holes for filling located in the electrodes, and to compare these characteristics with those of a similar design with holes in the side walls, Figure 3(b), hereinafter referred to as model B.

2. PHYSICAL AND MATHEMATICAL MODELS OF THE CELL

2.1. Physical model

Model A represents the physical model of the cell, which is the subject of this study. It consists of a glass tube with a length of L (m) and an internal diameter of D (m) and electrodes that are placed at the ends of the tube. Holes for filling the cell are located in the electrodes at a certain distance x (m) from the inner surface of the tube. Geometrical parameters x (m) and d (m) are identical for both ends of the cell, and the position of holes is centrally symmetrical to each other. The presence of holes results in a change in the effective cross-sectional area A (m^2), and, in agreement with equation (3), this leads to a change in the resistance of the liquid column and the occurrence of an error (bias) (2).

2.2. Mathematical model

So as to compute the resistance R_w (Ω) of the cell containing holes for filling, as in the previous study [11], COMSOL Multiphysics® software was used. This software implements the finite element method (FEM) [14] for solving the models, and

(a)

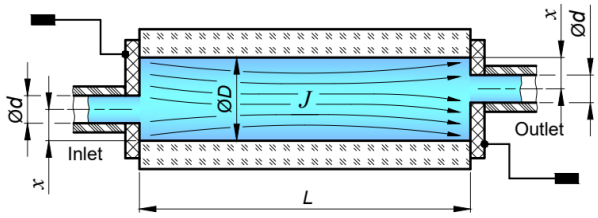

(b)

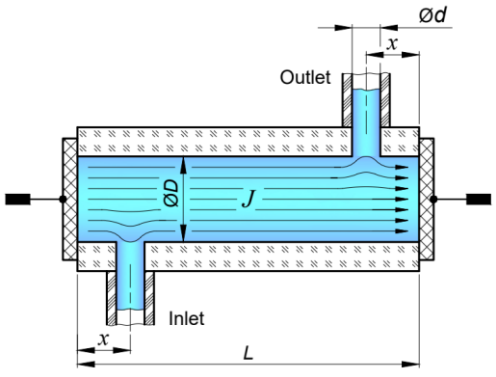

Figure 3. The physical models of the cells with inlet and outlet holes for filling (the current density lines are distorted due to the presence of holes).

calculations are carried out using two mathematical models. The first model describes the propagation of the electric field and corresponds to the three-dimensional Laplace's equation [15], [16]:

$$\frac{\partial^2 E}{\partial x^2}+\frac{\partial^2 E}{\partial y^2}+\frac{\partial^2 E}{\partial z^2}=0\,. \tag{4}$$

The second model, with the measuring direct current I_{cell} (A) through the cell set constant, is described as follows:

$$R_{\text{w}}=\frac{U_{\text{cell}}}{I_{\text{cell}}}=\frac{-\int_L E_z\,dL}{I_{\text{cell}}}, \tag{5}$$

where U_{cell} (V) is computed by integrating the z-component of the electric field strength E_Z (V·m^{-1}) over the liquid column length L (m).

When setting up the model, the following mandatory parameters were specified: direct current through the model I_{cell} = 1 mA, the EC of the solution k = 0.1 S·m^{-1}, the relative permittivity of the solution ε_r = 77 [17], and the temperature of the solution 25 °C. The contribution of fringe fields in the side quartz walls was neglected, so the boundaries of the model were electrically isolated, and the result of solving the model is the bulk resistance.

As for the mesh settings, predefined 'extremely fine' setting was used. Previous accuracy evaluations [11] show that this mesh setting ensures very high accuracy. The relative difference between the computed bulk resistance result and the value calculated using equation (3) does not exceed 0.002 % for the model dimensions considered in this work.

3. SIMULATION RESULTS

3.1. Dependencies for a range of geometric parameters

Based on the results of solving models with different geometric parameters L (mm) and D (mm), the dependencies of the electrical resistance bias δ_R (%) (2) for model A were obtained as functions of these parameters (Figure 4). The model with holes in the electrodes (model A) has a positive bias δ_R (%) in contrast to the model with side holes (model B) [11].

In order to compare the resistance biases δ_R (%) of model A and model B and find the difference in absolute values of the resistance biases Δ_δ (%), the following expression was used:

$$\Delta_\delta=\left|\delta_{\text{R,a}}\right|-\left|\delta_{\text{R,b}}\right|, \tag{6}$$

where $|\delta_{\text{R,a}}|$ (%) is the absolute value of the resistance bias for model A, and $|\delta_{\text{R,b}}|$ (%) is the absolute value of the resistance bias for model B.

Computation results show that for cells up to 100 mm long with a diameter $D \le 20$, the absolute bias value $|\delta_{\text{R,a}}|$ (%) of model A is 0.0005–0.007 % lower, according to equation (6), than the absolute bias value $|\delta_{\text{R,b}}|$ (%) of model B, given the same geometric parameters L (mm), D (mm), and d (mm). The position of the holes for model A is $x = D/2$ (mm), and for model B – 2 mm. In relative terms, this difference is 3–6 %. Therefore, this difference is not sufficiently large to make model A preferable to model B. A more important distinguishing feature of model A, compared to model B, is that the bias has a positive sign, in contrast to model B.

3.2. Influence of parameter *d* (mm)

The dependencies of the resistance bias δ_R (%) for cells of different lengths with diameters D = 10 mm and D = 20 mm are shown in Figure 5. The dependency plots show that the diameter of the holes for filling the cell has a significant effect on the cell resistance. When the diameter increases by 4 times, the resistance bias increases by 10–35 times, depending on the value of the D/d and L/D ratios.

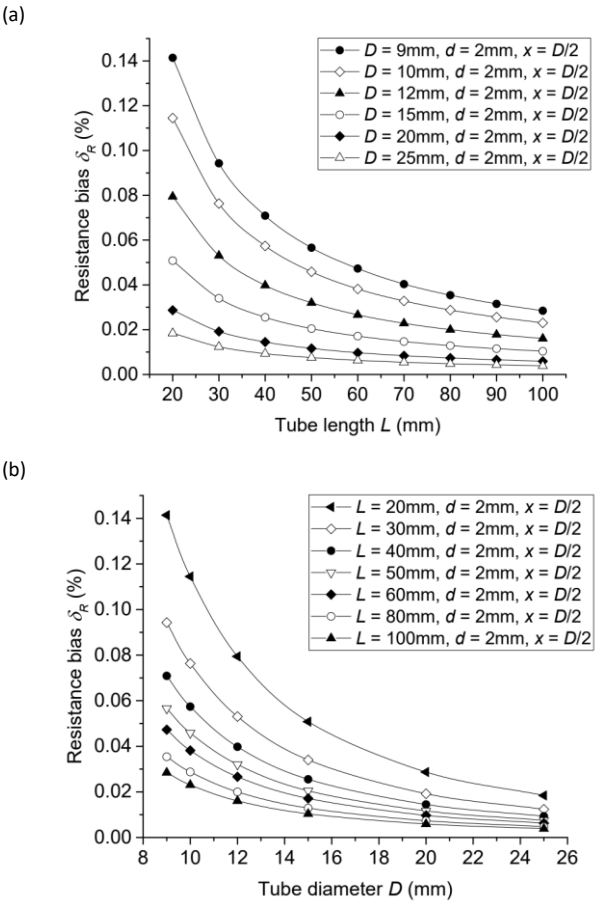

Figure 4. Dependencies of the resistance bias δ_R (%) for model A on various cell parameters.
(a) Resistance bias δ_R (%) as function of cell length L (mm);
(b) Resistance bias δ_R (%) as function of cell diameter D (mm);

Since the diameter of the holes significantly affects cell resistance, the task of making precision holes in the cell parts arises. For model A, when using metal electrodes, making a precision hole is relatively simple task. Freely available reamers allow for achieving tolerance limits of ±5 μm for diameters

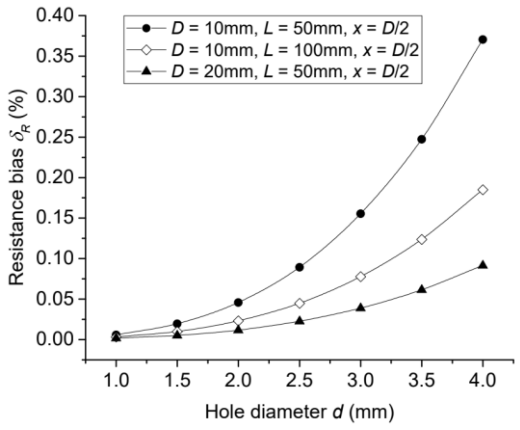

Figure 5. Dependencies of the resistance bias δ_R (%) of model A on hole diameter d (mm) at various geometric parameters.

(a)

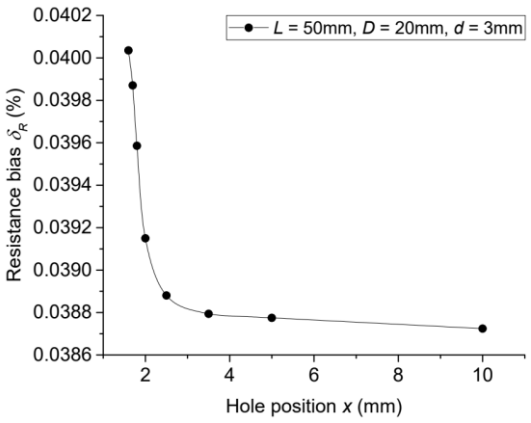

(b)

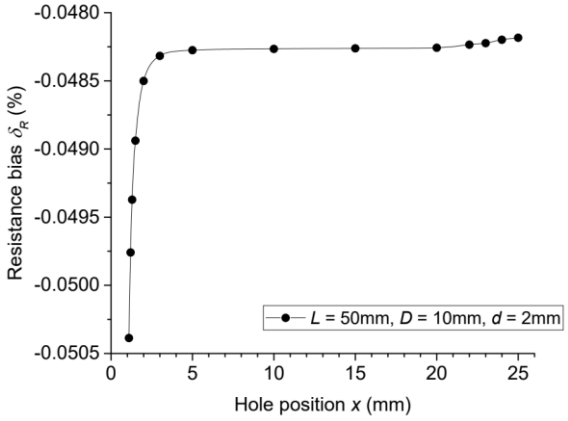

Figure 6. Dependencies of the resistance bias δ_R (%) on hole position x (mm).
(a) Plot for model A;
(b) Plot for model B.

between 0 and 3 mm, corresponding to international tolerance grade IT7. In contrast, for model B, making a hole in glass with the specified tolerance limits requires a special diamond mill, lapping tool, and a complex processing technique.

3.3. Influence of hole position *x* (mm)

The position x (mm) of the holes along the electrode as well as along the cell tube (for model B) has virtually no effect on the bias value δ_R (%). The plots (Figure 6) show that the change in cell resistance occurs in thousandths of a percent. The greatest effect on cell resistance for model A occurs when the holes are positioned right next to the tube wall, while the smallest effect is observed when the holes are located at the center of the electrode.

For model A, the hole positioning parameter x (m) is somewhat less controlled compared to model B. However, this issue can be resolved by making the electrodes the same diameter as the outer diameter of the glass tube. For example, both the electrodes and the glass tube can be inserted into a V-block made of dielectric material for optimal positioning. In this design, potential radial displacements of the electrodes would be minimal and can be measured using a dial indicator. The maximum observed radial displacement of an electrode could then be used in further model computations for uncertainty evaluations of the bias δ_R (%).

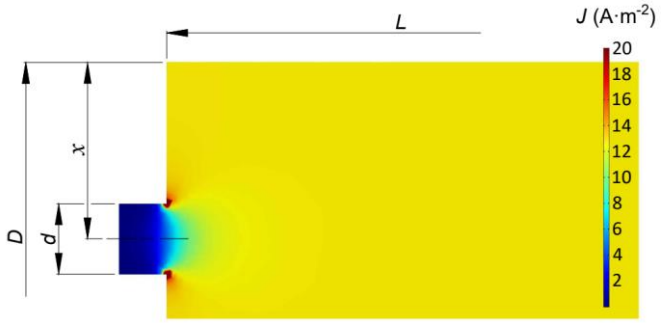

Figure 7. Current density distribution J (A·m^{-2}) in the central slice of the liquid column model near the inlet (D = 10 mm, d = 2 mm, L = 50 mm, $x = D/2$).

4. USING RESISTANCE BIAS DATA

The presence of holes for filling results in a significant change in the cell resistance and disrupts the non-uniformity of the current density J (A·m^{-2}) (see Figure 7). In model A, the presence of holes for filling reduces the effective cross-sectional area A (m^2) and increases the cell resistance, while in model B, the opposite is true: the effective cross-sectional area A (m^2) increases and the cell resistance decreases. However, these effects are constant. They can be eliminated by applying the resistance bias value δ_R (%) as a correction.

Estimating the resistance bias δ_R (%) for a cell of model A or B, with particular geometric parameters such as D (m), L (m), d (m), and x (m), makes it possible to calculate the EC measurement result and the constant K_{cell} (m^{-1}) for such a cell, which equals the L/A ratio.

By knowing the limit values of the diameter d (m) and the positioning parameter x (m), these values can be incorporated into further model computations to determine the limits of the bias δ_R (%). The resulting limit values can then be used to evaluate the uncertainty of the bias, assuming a uniform distribution.

Since the resistance biases δ_R (%) for models A and B have opposite signs, this property can also be utilized. For a cell with a hole in the electrode at one end and a hole in the cell wall at the other, the resistance bias δ_R (%) can be zero at specific geometric parameters L (m), D (m), d (m), and x (m). In such a case, the EC measurement result using this cell will correspond to that of the idealized model shown in Figure 2, with a uniform current density distribution inside.

5. CONCLUSIONS

Summarizing the results of the study on the effect of holes for filling in two-electrode cells, the following conclusions can be made. The presence of holes significantly affects the cell resistance, especially when the ratio D/d is reduced.

Regarding hole positioning, the error caused by positioning is 40–50 times smaller than the resistance bias introduced by the holes themselves. The shape of the liquid column in such cells remains fixed during measurements, ensuring that the resistance bias remains constant. For a cell of either model A or B with specific parameters D (m), L (m), d (m), and x (m), the bias value can be calculated and applied as a correction.

The resistance biases of models A and B are almost identical in absolute value when the geometric parameters D (m), L (m),

d (m), and x (m) are the same. The 3–6 % smaller bias in model A relative to model B is insignificant and does not indicate any substantial advantage for model A. The main distinction between the two models lies in the sign of the resistance bias: for model A, the bias is positive, while for model B, it is negative. This difference allows for the design of a hybrid cell model where there is a hole in the electrode on one side and a hole in the wall on the other. In such a cell, with certain geometric parameters, the resistance bias will be zero, and the measured EC result will correspond to that of an ideal cell with a uniform current density distribution, as shown in Figure 2.

After considering physical models A and B as potential designs for primary cells, the author concludes that model A, using metal electrodes, is the easiest to implement. Creating precise holes in metal electrodes with a given tolerance is a relatively simple task that does not require the specialized diamond tools or complex machining techniques necessary for model B. To better control the parameter x (m) in model A, the electrode could be made with the same diameter as the outer diameter D (m) of the cell tube. In this case, it will even be possible to estimate the acceptable limits within which the parameter x (m) is located using a dial indicator.

REFERENCES

[1] R. H. Shreiner, K. W. Pratt, Standard reference materials: Primary standards and standard reference materials for electrolytic conductivity, in: NIST Special Publication 260-142., 2004 Ed. U.S. Government Printing Office, Washington, 2004.

[2] C. Thirstrup, L. Deleebeeck, Review on electrolytic conductivity sensors, IEEE Trans. Instrum. Meas. 70 (2021), pp. 1–22. DOI: 10.1109/tim.2021.3083562

[3] T. Asakai, I. Maksimov, S. Onuma, T. Suzuki, T. Miura, A. Hioki, New Japanese certified reference materials for electrolytic conductivity measurements, Accreditation Qual. Assur. 22 (2017), pp. 73–81. DOI: 10.1007/s00769-017-1253-0

[4] E. Orrù, F. Durbiano, M. Ortolano, Reference measurement system for low electrolytic conductivity values with a flowing solution, Meas. Sci. Technol. 24 (2013), art. 035903, 6 pp. DOI: 10.1088/0957-0233/24/3/035903

[5] E. Orrù, Traceability of electrolytic conductivity measurements for ultra pure water. PhD thesis (2014). DOI: 10.6092/polito/porto/2553145

[6] F. Brinkmann, N. E. Dam, E. Deák, F. Durbiano, E. Ferrara, J. Fűkő, H. D. Jensen, M. Máriássy, (+ 5 more author), Primary methods for the measurement of electrolytic conductivity, Accreditation Qual. Assur. 8 (2003), pp. 346–353. DOI: 10.1007/s00769-003-0645-5

[7] P. Spitzer, S. Seitz, Electrolytic conductivity, in: Handbook of metrology and testing. H. Czichos, T. Saito, L. Smith. Springer, Heidelberg, 2011, ISBN: 978-3-642-16640-2, pp. 498–507.

[8] I. C. S. Fraga, P. P. Borges, B. S. R. Marques, W. B. S. Junior, S. P. Sobral, C. M. Ribeiro, J. C. Dias, J. C. Lopes, (+ 1 more author), Primary Measurements of Electrolytic Conductivity in Brazil, Proc. of Simposio de Metrología 2008, Santiago de Querétaro, México, 22 – 24 October 2008.

[9] I. C. S. Fraga, J. C. Lopes, L. R. Cordeiro, L. F. Silva, P. P. Borges, Evaluation of the stability of solutions of low electrolytic conductivity by primary measurements, J. Solution Chem. 44 (2015), pp. 1920–1936. DOI: 10.1007/s10953-015-0384-3

[10] K. C. Cunha, L. S. Pardellas, F. B. Gonzaga, Stability monitoring of electrolytic conductivity reference materials under repeated use conditions by the primary measurement method, J. Solution Chem. 49 (2020), pp. 306–315. DOI: 10.1007/s10953-020-00961-9

[11] O. Stennik, O. Mikhal, Resistance bias estimation of a liquid column in a cylindrical conductivity cell with lateral liquid supply, Eng. Res. Express 6 (2024), 015079. DOI: 10.1088/2631-8695/ad1f12

[12] Y. C. Wu, K. W. Pratt, W. F. Koch, Determination of the absolute specific conductance of primary standard KCl solutions, J. Solution Chem. 18 (1989), pp. 515–528. DOI: 10.1007/bf00664234

[13] O. Mikhal, D. Meleshchuk, O. Stennik, Methodological errors due to a non-cylindrical surface in a Jones-type cell with a removable central extension tube, Acta IMEKO 12 (2023) 4, article 24, 6 pp. DOI: 10.21014/actaimeko.v12i4.1604

[14] D. W. Pepper, J. C. Heinrich, The finite element method: Basic concepts and applications with MATLAB, MAPLE, and COMSOL, Third Edition. Taylor & Francis Group, Boca Raton, 2017, ISBN-13: 978–1–4987–3860–6, 628 pp. DOI: 10.1201/9781315395104

[15] S. Seitz, A. Manzin, H. D. Jensen, P. T. Jakobsen, P. Spitzer, Traceability of electrolytic conductivity measurements to the International System of Units in the sub mSm^{-1} region and review of models of electrolytic conductivity cells, Electrochim. Acta 55 (2010), pp. 6323-6331. DOI: 10.1016/j.electacta.2010.06.008

[16] A. Manzin, O. Bottauscio, D. P. Ansalone, Application of the thin-shell formulation to the numerical modeling of Stern layer in biomolecular electrostatics, J. Comput. Chem. 32 (2011), pp. 3105-3113. DOI: 10.1002/jcc.21896

[17] T. Chen, G. Hefter, R. Buchner, Dielectric Spectroscopy of Aqueous Solutions of KCl and CsCl, J. Phys. Chem. A 107 (2003), pp. 4025–4031. DOI: 10.1021/jp026429p